

Bayesian Probabilistic Numerical Methods for Industrial Process Monitoring

Chris. J. Oates*

School of Mathematics and Statistics, Newcastle University

Alan Turing Institute

and

Jon Cockayne

Department of Statistics, University of Warwick

and

Robert G. Aykroyd

School of Mathematics, University of Leeds

Abstract

The use of high-power industrial equipment, such as large-scale mixing equipment or a hydrocyclone for separation of particles in liquid suspension, demands careful monitoring to ensure correct operation. The task of monitoring the liquid suspension can be posed as a time-evolving inverse problem and solved with Bayesian statistical methods. In this paper, we extend Bayesian methods to incorporate statistical models for the error that is incurred in the numerical solution of the physical governing equations. This enables full uncertainty quantification within a principled computation-precision trade-off, in contrast to the over-confident inferences that are obtained when numerical error is ignored. The method is cast with a sequential Monte Carlo framework and an optimised implementation is provided in `Python`.

*Correspondence should be addressed to the first author. Chris. J. Oates is Senior Lecturer, School of Mathematics and Statistics, Newcastle University, NE1 7RU, UK and Group Leader, Lloyds Register Foundation Programme on Data-Centric Engineering, Alan Turing Institute, London NW1 2DB, UK. (E-mail: chris.oates@ncl.ac.uk) Jon Cockayne is a PhD student, Department of Statistics, University of Warwick, CV4 7AL, UK. (E-mail: j.cockayne@warwick.ac.uk) Robert G. Aykroyd is Senior Lecturer, School of Mathematics, University of Leeds, LS2 9JT, UK. (E-mail: r.g.aykroyd@leeds.ac.uk) This research was supported by the Australian Research Council Centre of Excellence for Mathematical and Statistical Frontiers and by the Key Technology Partnership program at the University of Technology Sydney. This material was based upon work partially supported by the National Science Foundation under Grant DMS-1127914 to the Statistical and Applied Mathematical Sciences Institute. Any opinions, findings, and conclusions or recommendations expressed in this material are those of the author(s) and do not necessarily reflect the views of the National Science Foundation.

Keywords: Inverse Problems, Electrical Tomography, Partial Differential Equations, Probabilistic Meshless Methods, Sequential Monte Carlo

1 Introduction

The goal of uncertainty quantification, based on indirect observation of a physical process of interest, is well studied and yet remains under-developed (Sullivan 2015). This is due in considerable part to the computational demands that are posed by the repeated solution of physical governing equations (the *forward problem*) in evaluation of the statistical likelihood. Probabilistic numerics (Hennig et al. 2015) is an emergent research field that aims to model the uncertainty in the solution space of the physical equations that arises when the forward problem is only approximately solved. In contrast to conventional emulation methods (Kennedy & O’Hagan 2001), which are *extrusive* in the sense that the physical equations are treated as a black-box, probabilistic numerical methods are *intrusive* and seek to model the error introduced in the numerical solution due to discretisation of the original continuous physical equations. Thus a probabilistic numerical method provides *uncertainty quantification for the forward problem* that is meaningful, reflective of the specific discretisation scheme employed, and enables a principled computation-precision trade-off, where the presence of an unknown discretisation error is explicitly accounted for by marginalisation over the unknown solution to the forward problem (Conrad et al. 2017, Briol et al. 2016). This paper contributes a rigorous assessment of probabilistic numerical methods for the Bayesian solution of an important inverse problem in industrial process monitoring, detailed next.

1.1 Industrial Hydrocyclone Equipment

Hydrocyclones provide a simple and inexpensive method for removing solids from liquids, as well as separating two liquids according to their relative densities (assuming equal fluid resistances) (Gutierrez et al. 2000). They have widespread applications, including in areas such as environmental engineering and the petrochemical industry (Sripriya et al. 2007). In particular, they have few moving parts, can handle large volumes and are relatively inexpensive to maintain. This makes them ideal as part of a continuous process in hazardous industrial settings and contrasts with alternatives, such as filters and centrifuges, which are more susceptible to breakdown and/or have higher running costs. The physical principles governing the hydrocyclone are simple; a mixed input is forced into a cone-shaped tank at high pressure, to create a circular rotation. This rotation forces less-dense material to the centre and denser material to the periphery of the tank. The less-dense material in the core can then be extracted from the top (overflow) and the denser material removed from the bottom of the tank (underflow). This mechanism is illustrated in Fig. 1.

Continual monitoring of the hydrocyclone is essential in most industrial applications, since the input flow rate is an important control parameter that can be adjusted to maximise the separation efficiency of the equipment. In addition, the high pressures that are often

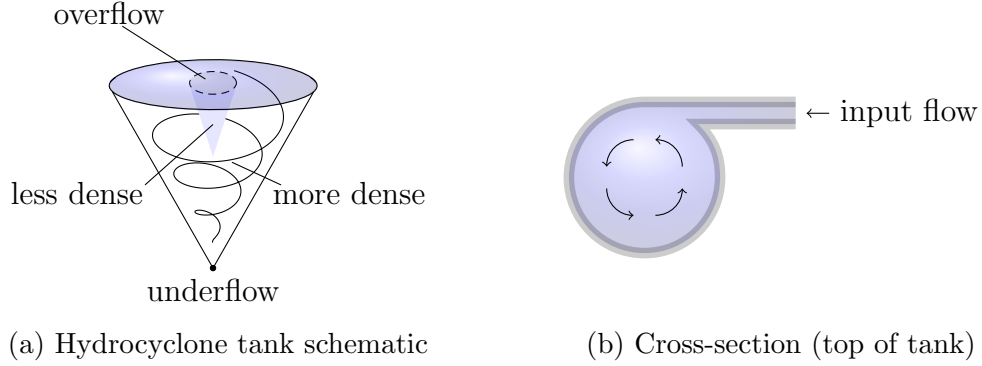


Figure 1: A simplified schematic description of typical hydrocyclone equipment. (a) The tank is cone-shaped with overflow and underflow pipes positioned to extract the separated contents. (b) Fluid, a mixture to be separated, is injected at high pressure at the top of the tank to create a vortex. Under correct operation, less-dense materials are directed toward the centre of the tank and denser materials are forced to the peripheries of the tank.

involved necessitate careful observation of the internal fluid dynamics to ensure safety in operation (Bradley 2013).

1.2 Statistical Challenges

Direct observation of the internal flow of the fluids is difficult or impossible due to, for example, the reinforced walls of the hydrocyclone and the opacity of the mixed component. Under correct operation, the output (overflow and underflow) can be monitored and tested for purity, but advanced indication of a potential loss of efficiency is desirable, if not essential in most industrial contexts. Such a warning allows for adjustment and hence avoidance of impending catastrophic failure. One possible technique for monitoring the internal flow is electrical impedance tomography (EIT). The target of an EIT analysis is the electrical conductivity field a^\dagger of the physical object; the conductivities of different fluid components will in general differ and this provides a means to measure the fluid constituents. This technique has many applications in medicine, as well as industry, as it provides a non-invasive method to estimate internal structure from external measurements (the *inverse problem*) (Gutierrez et al. 2000). Further, it is ideal for industrial processes as it is possible to collect data at rates of several hundred frames per second, hence allowing real-time monitoring and control of sensitive systems. The rapid acquisition of data requires equally rapid analysis. The nature of EIT modelling means that low-accuracy approximations to the physical governing equations may be needed to keep pace with incoming data. However, in standard approaches, the error introduced by a crude discretisation of the physical governing equations is ignored and leads to an over-optimistic view of the precision of results. This could lead to misleading interpretations of the results and hence potentially dangerous mis-control; it is therefore important to account for the presence of an unknown and non-negligible discretisation error in interpretation of the statistical output.

1.3 Our Contributions

The Bayesian approach to inverse problems is well-studied (Stuart 2010, Nouy & Soize 2014) and in particular the application of these statistical methods to EIT is now well-understood (Kaipio et al. 1999, 2000, Watzenig & Fox 2009, Dunlop & Stuart 2016, Yan & Guo 2015, Aykroyd 2015, Stuart & Teckentrup 2016) with sophisticated computational methods proposed (Kaipio et al. 2000, Vauhkonen et al. 2001, Polydorides & Lionheart 2002, Schwab & Stuart 2012, Schillings & Schwab 2013, Beskos et al. 2015, Chen & Schwab 2015, Hyvonen & Leinonen 2015, Chen & Schwab 2016*a,b,c*). In this paper, probabilistic numerical methods are proposed and investigated as a natural approach to uncertainty quantification with a computation-precision trade-off, wherein numerical error in the approximate solution of the forward problem is explicitly modelled and accounted for in a full Bayesian solution to the inverse problem of interest. At present, the literature on probabilistic numerical methods for partial differential equations consists of Owhadi (2015), Chkrebtii et al. (2016), Owhadi (2017), Owhadi & Zhang (2017), Cockayne et al. (2016*a,b*), Conrad et al. (2017), Raissi et al. (2017). This paper goes further than the most relevant work in Cockayne et al. (2016*a,b*), which tackled Bayesian inverse problems based on EIT with probabilistic numerical methods, in several aspects:

- The inversion problem herein is more challenging than considered in previous work, in that we aim to recover the temporal evolution of the unknown conductivity field a^\dagger based on indirect and noise-corrupted observations at a finite set of measurement times. To address this challenge, a Markovian prior model for a^\dagger is developed, which is shown to admit a filtering formulation (Todescato et al. 2017). This permits a sequential Monte Carlo method (particle filter) to be exploited for efficient data assimilation (Law et al. 2015).
- The filtering formulation introduces additional challenges due to the fact that numerical (discretisation) error in solution of the forward problem will be propagated through computations performed at earlier time points to later time points, as well as the possibility that numerical errors can accumulate within the computations. A detailed empirical investigation of the computation-precision trade-off is undertaken based on the use of probabilistic numerical methods for solution of the EIT governing equations. In particular, it is shown that the level of numerical precision required for the forward problem can be selected to match a prescribed level of statistical precision in the inverse problem through minimisation of an appropriate function of the posterior covariance function for a^\dagger . This provides a principled and statistically coherent approach to reduce the overall computational overhead.
- Real experimental data are analysed, generated by one of the present authors in a controlled laboratory experiment. These are used to demonstrate the efficacy of the approach under realistic experimental conditions.

In particular, this paper constitutes one of the first serious applications of probabilistic numerical methods to a challenging real-world problem, where proper quantification of

uncertainty is crucial.

1.4 Overview of the Paper

The structure of the paper is as follows: Sec. 2 contains the mathematical, statistical and computational methodological development. Sec. 3 reports our experimental results and Sec. 4 discusses their implications for further research and for future application to industrial processes.

2 Methods

In Sec. 2.1 we introduce the physical model and make the inversion problem formal. Then in Sec. 2.2 we recall the Bayesian approach to inversion, with an extension to a time-evolving unknown parameter. Sec. 2.3 introduces probabilistic models for numerical error incurred in discretisation of the physical governing equations. The final section, 2.5 develops a sequential Monte Carlo method for efficient computation.

2.1 Abstraction of the Inverse Problem

The physical governing equations and the measurement process are presented below, following the recent comprehensive treatment in Dunlop & Stuart (2016).

2.1.1 Set-Up

Consider a bounded, open domain $D \subset \mathbb{R}^d$ with smooth boundary denoted ∂D . Let $\bar{D} = D \cup \partial D$. The domain represents a physical object and our parameter of interest is the unknown conductivity field $a : \bar{D} \rightarrow \mathbb{R}$ of that object. Here $a(x)$ denotes the conductivity at spatial location $x \in \bar{D}$. Consider m electrodes fixed to ∂D , the region of contact being denoted $E_i \subset \partial D$. A current stimulation pattern $\mathbf{I} = (I_i)_{i=1}^m \in \mathbb{R}^m$ is passed, via the electrodes, through the object. Note that from physical conservation of current we have $\sum_{i=1}^m I_i = 0$.

The electrical potential $u : \bar{D} \rightarrow \mathbb{R}$ over the domain, induced by the current stimulation pattern, can be described by the following partial differential equation (PDE):

$$\begin{aligned} \nabla \cdot (a \nabla u) &= 0 \quad \text{in } D \\ \int_{E_i} a \nabla u \cdot \mathbf{n} d\sigma &= I_i \\ u + \zeta_i a \nabla u \cdot \mathbf{n} &= U_i \quad \text{on } E_i \\ a \nabla u \cdot \mathbf{n} &= 0 \quad \text{on } \partial D \setminus \cup_{i=1}^m E_i. \end{aligned} \tag{1}$$

Here \mathbf{n} is the *outward* unit normal, which corresponds to the convention that $I_i > 0$ refers to current flow *out* of the domain, and $d\sigma$ represents an infinitesimal boundary element.

The quantities U_i on the electrodes E_i will constitute the measurements. Known as the *complete electrode model* (CEM), this PDE was first studied in Cheng et al. (1989). In the CEM, each electrode is modelled as imperfect, as quantified by a contact impedances ζ_i , $i = 1, \dots, m$, here assumed known from a controlled experiment. Existence of a solution u is guaranteed and, under the additional condition that $\sum_{i=1}^m U_i = 0$, uniqueness of the solution u can also be established (Somersalo et al. 1992). Thus the forward problem is well-posed.

The true conductivity field $a = a^\dagger$ is considered to be unknown and is the object of interest. In contrast to most work on this problem, we consider that a is time-dependent and extend the notation as $a(x, t)$ for, with no loss in generality, a time index $t \in [0, 1]$. In order to estimate a^\dagger , measurements are obtained under distinct stimulation patterns $I_j \in \mathbb{R}^m$, $j = 1, \dots, m'$, of the form

$$y_{i,j,k} = \mathcal{P}_{i,j,k} u^\dagger + \epsilon_{i,j,k} \in \mathbb{R} \quad (2)$$

where the projections

$$\mathcal{P}_{i,j,k} u^\dagger := u(x_i^E; I_j, a^\dagger(\cdot, t_k)) + \zeta_i a^\dagger(x_i^E, t_k) \nabla u(x_i^E; I_j, a(\cdot, t_k)) \cdot \mathbf{n}(x_i^E),$$

are defined for each electrode i , each stimulation pattern j and each discrete time point t_k , $k = 1, \dots, n$. Here $u(\cdot; I, a)$ denotes the solution of the PDE with conductivity field a and stimulation pattern I , while x_i^E is a point central to the electrode E_i . Thus for fixed j, k , the vector $\mathcal{P}_{i,j,k} u^\dagger$ corresponds to the quantities U_i in the CEM with conductivity field $a = a^\dagger(\cdot, t_k)$ and stimulation pattern $I = I_j$. For the case of perfect electrodes ($\zeta_i = 0$), the projection $\mathcal{P}_{i,j,k}$ reduces to straight-forward evaluation of the potential field.

In the absence of further conditions on a , the inverse problem is ill-posed (Stuart 2010). Further, the PDE does not specify the time-evolution of the field $a(\cdot, t)$. To proceed, the inverse problem must therefore be regularised.

2.2 The Bayesian Approach to Inversion

In this section we exploit Bayesian methods to make the inverse problem well-posed. Sec. 2.2.1 introduces the prior model, Sec. 2.2.2 casts posterior computation as a filtering problem and Sec. 2.2.3 reviews mathematical analysis for numerical approximation of the posterior that accounts for numerical error in the PDE solution method.

2.2.1 Prior Model for the Conductivity Field

In this paper we interpret Eqn. 1 in the strong form, which in particular requires the existence of ∇a on D . This information will be encoded into a prior distribution: Let $\{\phi_i\}_{i=1}^\infty$ be an orthonormal basis for a separable Hilbert space H with norm $\|\cdot\|_H$. It is assumed that $H \subset C^1(\bar{D})$, where $C^m(S)$ is used to denote the set of m -times continuously differentiable functions from S to \mathbb{R} . Let $(\Omega, \mathcal{F}, \mathbb{P})$ be a probability space and for measurable $v : \Omega \rightarrow \mathbb{R}$ denote $\mathbb{E}v = \int v d\mathbb{P}$.

Model Assumption 1. Let $\alpha > 1/2$ and $\omega \in \Omega$. Our prior model is expressed as a separable Karhounen-Loéve expansion:

$$a(x, t; \omega) = \sum_{i=1}^{\infty} i^{-\alpha} \psi_i(t; \omega) \phi_i(x)$$

where the $\omega \mapsto \psi_i(\cdot; \omega)$ are modelled as independent Gaussian processes with mean functions $m_{\psi,i}$ and covariance functions $k_{\psi,i}$ such that

$$m_{\psi}^{\max} := \sup_{i \in \mathbb{N}} \sup_{t \in [0,1]} |m_{\psi,i}(t)| < \infty, \quad k_{\psi}^{\max} := \sup_{i \in \mathbb{N}} \sup_{t \in [0,1]} k_{\psi,i}(t, t) < \infty.$$

Henceforth the probability argument $\omega \in \Omega$ will be left implicit.

This prior construction ensures that ∇a exists in D . To see this, let $L_H^2 = \{v : \bar{D} \times \Omega \rightarrow \mathbb{R} \text{ s.t. } \mathbb{E} \|v\|_H^2 < \infty\}$, which is a Banach space with norm $(\mathbb{E} \|\cdot\|_H^2)^{1/2}$; see section 2.4 of Dashti & Stuart (2016). Then:

Proposition 1. For fixed $t \in [0, 1]$, almost surely $a(\cdot, t)$ exists in $C^1(\bar{D})$.

Proof. Following Thm. 2.10 in Dashti & Stuart (2016), consider the partial sums

$$a^N(\cdot, t) = \sum_{i=1}^N i^{-\alpha} \psi_i(t) \phi_i(\cdot).$$

For $N > M$ we have

$$\begin{aligned} \mathbb{E} \|a^N(\cdot, t) - a^M(\cdot, t)\|_H^2 &= \mathbb{E} \sum_{i=M+1}^N i^{-2\alpha} |\psi_i(t)|^2 \\ &\leq \sum_{i=M+1}^N i^{-2\alpha} [(m_{\psi}^{\max})^2 + k_{\psi}^{\max}] \leq [(m_{\psi}^{\max})^2 + k_{\psi}^{\max}] \sum_{i=M+1}^{\infty} i^{-2\alpha}. \end{aligned}$$

Since $\alpha > 1/2$, the RHS vanishes as $M \rightarrow \infty$. Thus, as L_H^2 is a Banach space, $a(\cdot, t)$ exists as an L_H^2 limit. It follows that $a(\cdot, t)$ takes values almost surely in $C^1(\bar{D})$. \square

Note that, in particular, this result justifies point evaluation of ∇a in the algorithms that we present; since $x \mapsto \nabla a(x, t)$ is almost surely continuous, such point evaluations are almost surely well-defined.

This paper imparts weak prior assumptions on the time-evolution of the random field:

Model Assumption 2. The ψ_i are modelled as Brownian with mean functions $m_{\psi,i}(t) = 0$ and covariance functions $k_{\psi,i}(t, t') = \lambda \min(t + \tau, t' + \tau)$, for all $t, t' \in [0, 1]$ and $\lambda > 0$, $\tau \geq 0$.

This prior model allows for flexible and data-driven estimation of the temporal evolution of the unknown conductivity field. At the same time, this choice allows estimation to be cast as a filtering problem (see Sec. 2.2.2) due to the following important fact:

Proposition 2 (Due to Wiener (1949)). *The increments $\psi_i(t+s) - \psi_i(t)$ are independent with distribution $N(0, \lambda(s+\tau))$, for all $0 \leq t \leq t+s \leq 1$.*

An immediate consequence is that the field $a(\cdot, t)$ itself is a Markov process. To see this, let

$$k_\phi(x, x') = \sum_{i=1}^{\infty} i^{-2\alpha} \phi_i(x) \phi_i(x').$$

Then:

Corollary 1. *The increments $a_\Delta(\cdot) := a(\cdot, t+s) - a(\cdot, t)$ are independent Gaussian random fields with mean function $m_\Delta(x) = 0$ and covariance function $k_\Delta(x, x') = \lambda(s+\tau)k_\phi(x, x')$, for all $x, x' \in D$ and all $0 \leq t \leq t+s \leq 1$.*

Proof. From direct algebra:

$$\begin{aligned} a_\Delta(x) &= a(x, t+s) - a(x, t) = \sum_{i=1}^{\infty} i^{-\alpha} [\psi_i(t+s) - \psi_i(t)] \phi_i(x) \\ &= \sqrt{\lambda(s+\tau)} \sum_{i=1}^{\infty} i^{-\alpha} \xi_i \phi_i(x) \end{aligned}$$

where the ξ_i are independent $N(0, 1)$. From the Karhounen-Loève theorem (Loève 1977), this is recognised as a Gaussian random field with mean function $m_\Delta(x) = 0$ and covariance function

$$\begin{aligned} k_\Delta(x, x') &= \lambda(s+\tau) \sum_{i=1}^{\infty} i^{-2\alpha} \phi_i(x) \phi_i(x') \\ &= \lambda(s+\tau) k_\phi(x, x'), \end{aligned}$$

as claimed. □

Let Γ_s denote the distribution of the increment a_Δ over the time interval $[t, t+s]$. For Γ_s we obtain the Radon-Nikodym derivative

$$\frac{d\Gamma_s}{d\gamma}(a_\Delta) \propto \exp\left(-\frac{1}{2}\|a_\Delta\|_{k_\Delta}^2\right) = \exp\left(-\frac{1}{2\lambda(s+\tau)}\|a_\Delta\|_{k_\phi}^2\right)$$

with respect to abstract Wiener measure γ (Gross 1967), where $\|\cdot\|_k$ denotes the Cameron-Martin norm based on the covariance function k .

2.2.2 Formulation as a Filtering Problem

Denote $a_k = a(\cdot, t_k) \in L_H^2$. Then the directed acyclic graph for the statistical model is as follows:

$$\begin{array}{ccccccc} a_1 & \rightarrow & a_2 & \rightarrow & \dots & \rightarrow & a_{n-1} & \rightarrow & a_n \\ \downarrow & & \downarrow & & & & \downarrow & & \downarrow \\ y_{\cdot,1} & & y_{\cdot,2} & & \dots & & y_{\cdot,n-1} & & y_{\cdot,n} \end{array}$$

Let Π_n represent the posterior distribution over the conductivity field based on the data $y_{\cdot,k}$ for $k \leq n$. Then statistical inference is naturally formulated as a filtering problem at linear cost (Särkkä 2013, Todescato et al. 2017):

$$\frac{d\Pi_n}{d\Pi_{n-1}}(a) \propto p(y_{\cdot,n} | \mathbf{I}, a(\cdot, t_n)).$$

Here the Radon-Nikodym notation has been used on the LHS, while p has the conventional interpretation as a p.d.f. with respect to Lebesgue measure, here representing the likelihood model specified by the distributional model for $\epsilon_{i,j,k}$ in Eqn. 2. The solution to the filtering problem is the n -step posterior distribution:

$$\frac{d\Pi_n}{d\Pi_0}(a) \propto \prod_{k=1}^n \frac{d\Pi_k}{d\Pi_{k-1}}(a)$$

where the reference measure Π_0 is the prior distribution for the conductivity field given in Assumption 1. From Prop. 2, the prior marginal on (a_1, \dots, a_n) , denoted $\Pi_{0,1:n}$, can be decomposed as follows:

$$\frac{d\Pi_{0,1:n}}{d(\gamma \times \dots \times \gamma)}(a_1, \dots, a_n) \propto \frac{d\Pi_{0,1}}{d\gamma}(a_1) \prod_{k=2}^n \frac{d\Gamma_{t_k - t_{k-1}}}{d\gamma}(a_k - a_{k-1}),$$

where $\gamma \times \dots \times \gamma$ denotes the product of n abstract Wiener measures and the initial distribution $\Pi_{0,1}$ is computed as

$$\frac{d\Pi_{0,1}}{d\gamma}(a_1) \propto \exp\left(-\frac{1}{2\lambda(t_1 + \tau)} \|a_1\|_{k_\phi}^2\right)$$

as a direct consequence of Assumption 2. Later we use $\Pi_{n,n+1}$ to denote the marginal of Π_n over the components $a(\cdot, t_{n+1})$; the so-called *posterior predictive* distribution. This is of industrial relevance since it allows anticipation of the future dynamics and thus for intelligent hazard control.

2.2.3 Numerical Error and its Analysis

The likelihood model in Eqn. 2 depends on the projections $\mathcal{P}_{i,j,k}u$ which in turn depend on the exact solution $u(x_i^E; \mathbf{I}_j, a(\cdot, t_k))$ of the PDE for given inputs \mathbf{I}_j and $a(\cdot, t_k)$. In general

the exact solution of the PDE is unavailable in closed-form and numerical methods are used to obtain discrete approximations

$$u(x; a, \mathbf{I}) \approx \sum_{l=1}^L \beta_l \varphi_l(x), \quad \beta_1, \dots, \beta_L \in \mathbb{R},$$

for instance based on a finite element or collocation basis $\{\varphi_l\}_{l=1}^L$ (Quarteroni & Valli 2008). The assessment of the error introduced through discretisation is well-studied, with sophisticated theories for worst-case and average-case errors and beyond (Novak & Wozniakowski 2008, 2010).

Several papers have leveraged these analyses to consider the impact of discretisation error in the forward problem on the inferences that are made for the inverse problem (Schwab & Stuart 2012, Schillings & Schwab 2013, 2014, Nouy & Soize 2014, Bui-Thanh & Ghattas 2014, Chen & Schwab 2015, 2016*c,a*, Nagel & Sudret 2016). These analyses all focus on static inverse problems (i.e. for a single time point). However, the generalisation of these theoretical results to the temporal context introduces considerable technical difficulties. Indeed, the filtering formulation is such that error in an approximation Π'_1 of Π_1 will be propagated and lead to an error in the approximation Π'_n of Π_n whenever $n \geq 2$. Numerical approximation of Π_n thus involves $n - 1$ sources of discretisation error and analysis in the time-evolving setting must account for propagation and accumulation of these discretisation errors. However, standard worst-case error analyses (such as those listed above) are inappropriate for temporal problems, since in general the worst-case scenario will not be realised simultaneously by all numerical methods involved in the computational work-flow.

Presented with such an inherently challenging problem, our novel approach - described in the next section - to *model* discretisation error as an unknown random variable and propagate *uncertainty due to discretisation* through computation has appeal on philosophical, technical and practical levels.

2.3 Probabilistic Numerical Methods

Recall that the exact solution $u(\cdot; a, \mathbf{I})$ to the PDE is unavailable in closed-form. In this section we view numerical solution of Eqn. 1 not as a forward problem, but as an inverse problem in its own right (called a *sub-inverse* problem in this work) and provide full quantification of solution uncertainty that arises from the discretisation of this PDE via a collocation-type method. Sec. 2.3.1 introduces a prior model for u while Sec. 2.3.2 completes the specification of this sub-inverse problem associated with solution of the PDE. Then, Sec. 2.3.3 demonstrates how solution uncertainty can be propagated through the original inverse problem by marginalisation over the unknown exact solution u of the PDE. Sec. 2.4 establishes theoretical properties of the proposed method.

2.3.1 Prior Model for the Potential Field

In this section we again adopt Bayesian methods to make the sub-inverse problem well-posed. The chief task is to construct a prior for u , the potential field. In principle, the

physical governing equations, together with the prior for the conductivity field a , induce a unique prior for the potential field. The relationship between these probabilities has been explored in the context of stochastic PDEs; see Lord et al. (2014) for a book-length treatment. However, the task of characterising (or even approximating) the implied distribution on u is highly non-trivial¹. For this reason, we follow Cockayne et al. (2016a,b) and treat the two unknown fields as independent under the prior model. In particular, we encode independence across time points into the prior model for u , a choice that is algorithmically convenient. This allows us, in the following, to leave the time index implicit. This has a natural statistical interpretation of encoding only partial information into the prior - and can be both statistically and pragmatically justified (Potter & Anderson 1983).

To reduce notation in this and the following section, we consider a fixed conductivity field $a \in C^1(\bar{D})$ and a fixed current stimulation pattern $I \in \mathbb{R}^m$; these will each be left implicit.

Model Assumption 3. *The unknown solution u to Eqn. 1 is modelled as a Gaussian process with mean function $m_u(x) = 0$ and covariance function*

$$k_u(x, x') = \int k_u^0(x, z) k_u^0(z, x') dz \quad (3)$$

such that $k_u^0 \in C^{2 \times 2}(\bar{D} \times \bar{D})$ is a positive-definite kernel.

This minimal assumption ensures that, *under the prior*, the differential $\nabla \cdot (a \nabla u)$ is well-defined over D . Indeed:

Proposition 3. *Almost surely $u \in C^2(\bar{D})$.*

Proof. Let $H(k)$ denote the reproducing kernel Hilbert space associated with a kernel k . In Cialenco et al. (2012), Lemma 2.2, it was established that a generic integral-type kernel k_u , as in Eqn. 3, corresponds to the covariance function for a Gaussian process that takes values almost surely in $H(k_u^0)$. To complete the proof, Corr. 4.36 (p131) in Steinwart & Christmann (2008) establishes that if $k_u^0 \in C^{2 \times 2}(\bar{D} \times \bar{D})$ then $H(k_u^0) \subset C^2(\bar{D})$. \square

2.3.2 Probabilistic Meshless Method

Next we obtain a posterior distribution over the solution u to the PDE in Eqn. 1. In particular this requires us to be explicit about the nature of our “data” for this sub-inverse problem. The mathematical justification for our approach below is provided in the information-based complexity literature on linear elliptic PDEs of the form $Au = f$ on D , $Bu = g$ on ∂D (Werschulz 1996, Novak & Wozniakowski 2008, Cialenco et al. 2012). In this framework, limited data $f_i = f(x_i^A)$, $g_i = g(x_i^B)$ are provided on the forcing term f and the boundary term g ; the mathematical problem is then optimal recovery of the solution u from these data, under a loss function that must be specified. This is a particular example

¹In principle this requires knowledge of the Green’s function of the PDE, but if this was known we would not have needed to discretise the PDE.

of a *linear information* problem, since the f_i and g_i are linear projections of the unknown solution u of interest; see Novak & Wozniakowski (2008) for a book length treatment.

The data with which we work, in the above sense, are linear projections obtained at *collocation* points $\{x_i^A\}_{i=1}^{n_A} \subset D$ and $\{x_i^B\}_{i=1}^{n_B} \subset \partial D$:

$$\begin{aligned}\mathcal{L}_i u &:= \nabla \cdot a(x_i^A) \nabla u(x_i^A) &= 0 & i = 1, \dots, n_A \\ \mathcal{L}_{n_A+i} u &:= a(x_i^B) \nabla u(x_i^B) \cdot \mathbf{n}(x_i^B) &= 0 & i = 1, \dots, n_B \\ \mathcal{L}_{n_A+n_B+i} u &:= \int_{E_i} a \nabla u \cdot \mathbf{n} d\sigma &= I_i & i = 1, \dots, m.\end{aligned}$$

Here $\mathcal{L} = [\mathcal{L}_1, \dots, \mathcal{L}_{n_A+n_B+m}]$ is a linear operator from $C^2(\bar{D})$ to $\mathbb{R}^{n_A+n_B+m}$. For a function $h(\cdot, \cdot) \in C^{2 \times 2}(\bar{D} \times \bar{D})$, in a slight abuse of notation, $\mathcal{L}h$ will be used to denote action of \mathcal{L} on the first argument, while the notation $\bar{\mathcal{L}}h$ denotes action on the second argument. The composition $\mathcal{L}\bar{\mathcal{L}}h$ is understood as a matrix with (i, j) th element $\mathcal{L}_i \bar{\mathcal{L}}_j h \in \mathbb{R}$. In this notation, the data can be expressed as $\mathcal{L}u = [0^\top, \mathbf{I}^\top]^\top$ where $\mathbf{I} = [I_1, \dots, I_m]^\top$. The posterior over u is obtained by conditioning the prior measure on these data. Denote $\mathcal{P} = [\mathcal{P}_1, \dots, \mathcal{P}_m]^\top$ the projections

$$\mathcal{P}_i u := u(x_i^E) + \zeta_i a(x_i^E) \nabla u(x_i^E) \cdot \mathbf{n}(x_i^E).$$

For our purposes, it is sufficient to obtain the posterior over the finite dimensional vector $\mathcal{P}u$:

$$\begin{aligned}\mathcal{P}u \Big| \mathcal{L}u = \begin{bmatrix} 0 \\ \mathbf{I} \end{bmatrix} &\sim \mathcal{N}(\mu, \Sigma) \\ \mu &= [\mathcal{P}\bar{\mathcal{L}}k_u][\mathcal{L}\bar{\mathcal{L}}k_u]^{-1} \begin{bmatrix} 0 \\ \mathbf{I} \end{bmatrix} \\ \Sigma &= [\mathcal{P}\bar{\mathcal{P}}k_u] - [\mathcal{P}\bar{\mathcal{L}}k_u][\mathcal{L}\bar{\mathcal{L}}k_u]^{-1}[\mathcal{L}\bar{\mathcal{P}}k_u]\end{aligned}\tag{4}$$

This distribution represents uncertainty due to the finite amount of computation that is afforded to numerical solution of the PDE in Eqn. 1. Eqn. 4 was termed a *probabilistic meshless method* in Cockayne et al. (2016a,b). Note that the *maximum a posteriori* estimate for u is identical to the point estimate provided by symmetric collocation (Fasshauer 1996) and this point estimator (only) was considered in the context of Bayesian PDE-constrained inverse problems in Marzouk & Xiu (2009), Yan & Guo (2015). Considerable theoretical advances in the numerical analysis of these probabilistic numerical methods (for static problems) have since been made in Owhadi (2017). For non-degenerate kernels k_u , the matrix $\mathcal{L}\bar{\mathcal{L}}k_u$ is of full rank provided that no two collocation points are coincidental. The selection of collocation points can be formulated as a problem of statistical experimental design; see Cockayne et al. (2016a).

2.3.3 Marginal Likelihood

The natural approach to define a data distribution is through marginalisation over the unknown solution u to the PDE. This marginalisation can be performed in closed form under a Gaussian measurement error model:

Model Assumption 4. *The measurement errors $\epsilon_{i,j,k}$ are independent $N(0, \sigma^2)$.*

Consider a stimulation pattern I_j applied at time $t_k \in [0, 1]$. Define $P_{j,k} = \mathcal{P}u(\cdot; I_j, a(\cdot, t_k))$ and denote by μ_j, Σ_j the output of the probabilistic meshless method (Eqn. 4) for the input stimulation pattern I_j . Then the marginal distribution of the data $y_{\cdot,j,k}$, given the measurement error standard deviation σ , admits a density as follows:

$$\begin{aligned} p^*(y_{\cdot,j,k} | I_j, a(\cdot, t_k), \sigma) &= \int N(y_{\cdot,j,k} | P_{j,k}, \sigma^2 I) N(P_{j,k} | \mu_j, \Sigma_j) dP_{j,k} \\ &= N(y_{\cdot,j,k} | \mu_j, \sigma^2 I + \Sigma_j) \end{aligned} \quad (5)$$

where we have used the shorthand of $N(\cdot | \mu_j, \Sigma_j)$ for the p.d.f. of $N(\mu_j, \Sigma_j)$. Eqn. 5 has the clear interpretation of inflating the measurement error covariance $\sigma^2 I$ by an additional amount Σ_j to reflect additional uncertainty due to discretisation error in the numerical solution of the PDE in Eqn. 1. This distinguishes the probabilistic approach from other applications of collocation methods in the solution of Bayesian PDE-constrained inverse problems, where uncertainty due to discretisation is ignored (Marzouk & Xiu 2009, Yan & Guo 2015). Eqn. 5 also appears in the emulation literature for static problems (e.g. Calvetti et al. 2017). However, emulation methods treat the PDE as a perfect black-box and, as a result, the matrices Σ_j obtained from emulation do not reflect the fact that the PDE must be discretised².

This paper proposes to base statistical inferences on the posterior distribution Π_n^* defined recursively via

$$\frac{d\Pi_n^*}{d\Pi_{n-1}^*}(a) \propto p^*(y_{\cdot, \cdot, n} | I, a(\cdot, t_n), \sigma), \quad \Pi_0^* = \Pi_0.$$

In particular we will be most interested in the posterior predictive distribution $\Pi_{n,n+1}^*$ obtained with these probabilistic numerical methods, where discretisation uncertainty is explicitly modelled. Unlike $\Pi_{n,n+1}$, the posterior predictive distribution $\Pi_{n,n+1}^*$ can be exactly computed, since it does not require the exact solution of the PDE.

2.4 Theoretical Properties

Consider the case in which the contact impedances are considered to be negligible; $\zeta_i = 0$. Then the projections $\mathcal{P}u = [u(x_1^E), \dots, u(x_m^E)]^\top$ are direct evaluations of the solution u to the PDE in Eqn. 1. In this case the theoretical analysis of Cockayne et al. (2016a) can be exploited to assess the consistency of the probabilistic meshless method.

Define the *fill distance* $h := \min\{h_A, h_B\}$ where $h_A = \sup_{x \in D} \min_i \|x - x_i^A\|_2$ and $h_B = \sup_{x \in \partial D} \min_i \|x - x_i^B\|_2$. Then we outline the following result:

Proposition 4. *Let B_ϵ denote a Euclidean ball of radius $\epsilon > 0$ centred on the true projection $\mathcal{P}u$ in \mathbb{R}^m . Then, under the assumptions of Cockayne et al. (2016a), which include that*

²The typical usage of emulators is to reduce the total number of forward problems that must be solved. This consideration is orthogonal to the present work and the two approaches could be combined.

$H(k_u^0)$ is norm-equivalent to the Sobolev space $H^\beta(D)$, then the mass afforded to $\mathbb{R}^m \setminus B_\epsilon$ in the posterior $N(\mu_j, \Sigma_j)$ is $O(\epsilon^{-2}h^{2\beta-4-d})$ for $h > 0$ sufficiently small.

Proof. Let $\mu(x)$ and $\sigma(x)$ denote, respectively, the posterior mean and standard deviation of $u(x)$ under the probabilistic meshless method. Prop. 4.1 of Cockayne et al. (2016a) established that the posterior mean $\mu(x)$ satisfies $|\mu(x) - u(x)| \leq \sigma(x)\|u\|_{H(k_u)}$ and Prop. 4.2 of Cockayne et al. (2016a) established that the posterior standard deviation $\sigma(x)$ satisfies $\sigma(x) \leq Ch^{\beta-2-d/2}$ for some constant C independent of $x \in D$. In particular we have $\|\mu_j - \mathcal{P}u\|_2 = O(h^{\beta-2-d/2})$. Lastly, Thm. 4.3 of Cockayne et al. (2016a) established a generic rate of contraction for the mass of a Gaussian distribution of $O(\epsilon^{-2}h^{2\beta-4-d})$, as required. (Note that these results are specific consequences of more general results found in Lem. 3.4 in Cialenco et al. (2012) and Secs. 11.3 and 16.3 of Wendland (2005).) \square

This result ensures asymptotic agreement between the probabilistic numerical approach to the inverse problem and the (unavailable) exact approach based on the exact solution of the PDE in Eqn. 1 in the limit $h \rightarrow 0$ of infinite computation. Empirical evidence for the appropriateness of the uncertainty quantification for static EIT experiments and finite computation was presented in Cockayne et al. (2016a).

2.5 Computation via Sequential Monte Carlo

The filtering formulation of Sec. 2.2.2 suggests a natural approach to computation based on particle filters, otherwise known as sequential Monte Carlo (SMC) methods (Del Moral 2004). Note that our use of SMC, in the context of inference for a time-evolving unknown field, is distinct from Kantas et al. (2014), Beskos et al. (2015), who considered SMC methods for the solution of a static inverse problem with an artificial sequence of tempered distributions.

Let $\Pi_{0,1} \ll \Pi'_{0,1}$ where $\Pi'_{0,1}$ is a user-chosen importance distribution on $C^1(\bar{D})$ (and could be Π_0). The method begins with N independent draws $a_0^{(1)}, \dots, a_0^{(N)}$ from $\Pi'_{0,1}$; each draw $a_0^{(i)}$ is associated with an importance weight

$$w_0^{(i)} \propto \frac{d\Pi_{0,1}}{d\Pi'_{0,1}}(a_0^{(i)})$$

such that $\sum_{i=1}^N w_0^{(i)} = 1$. This provides an empirical approximation $\sum_{i=1}^N w_0^{(i)} a_0^{(i)}$ to the prior marginal distribution $\Pi_{0,1}$ that becomes exact as N is increased. Let $t_0 := t_1$. Then, at each iteration $n = 1, 2, \dots$ of the SMC algorithm, the following steps are performed:

1. **Re-sample:** Particles $\tilde{a}_n^{(1)}, \dots, \tilde{a}_n^{(N)}$ are generated as a random sample (with replacement) of size N from the empirical distribution $\sum_{i=1}^N w_{n-1}^{(i)} a_{n-1}^{(i)}$.
2. **Move:** Each particle $\tilde{a}_n^{(i)}$ is updated to $a_n^{(i)}$ according to a Markov transition M_{n-1} that leaves Π_{n-1}^* invariant. (See Cotter et al. (2013) for several examples of such Markov kernels on Hilbert spaces.)

3. **Re-weight:** The next set of weights are defined as

$$w_n^{(i)} \propto \frac{d\Pi_n^*}{d\Pi_{n-1}^*}(a_n^{(i)}) \frac{d\Gamma_{t_n-t_{n-1}}}{d\gamma}(a_n^{(i)} - \tilde{a}_n^{(i)})$$

and such that $\sum_{i=1}^N w_n^{(i)} = 1$.

The output after n iterations is an empirical approximation $\sum_{i=1}^N w_n^{(i)} a_n^{(i)}$ to the posterior distribution Π_n^* . The posterior predictive distribution $\Pi_{n,n+1}^*$ can be obtained from similar methods, as

$$\frac{d\Pi_{n,n+1}^*}{d\Pi_n^*}(a) \propto \frac{d\Gamma_{t_{n+1}-t_n}}{d\gamma}(a).$$

The re-sample step in the above procedure does not in general need to occur at each iteration, only when the effective sample size is small; see Del Moral (2004). Theoretical analysis of SMC methods in the context of infinite-dimensional state spaces is provided in Beskos et al. (2015). For this work we considered a fairly standard SMC method, but several extensions are possible and include, in particular, stratified or quasi Monte Carlo re-sampling methods (Gerber & Chopin 2015). One extension which we explored was to introduce fictitious intermediate distributions between Π_{n-1}^* and Π_n^* following Chopin (2002), which we found to improve the performance of SMC in this context. For the experiments reported in the paper, 100 intermediate distributions were used, defined by tempering on a linear temperature ladder, c.f. Kantas et al. (2014), Beskos et al. (2015).

This completes our methodological development. Optimised `Python` scripts are available to reproduce these results at: https://github.com/jcockayne/hydrocyclone_code. Next, we report empirical results based on data from a controlled EIT experiment.

3 Results

This section considers data from a laboratory experiment designed to investigate the temporal mixing of two liquids. The experiment was conducted by one of the present authors and carefully controlled, to enable assessment of statistical methods and to mimic the salient features of industrial hydrocyclone equipments.

3.1 Experimental Protocol

In the experiment, a cylindrical perspex tank of diameter 15cm and height 30cm was used with a single ring of $m = 8$ electrodes, each measuring approximately 1cm wide by 3cm high. The electrodes start at the bottom of the tank, with the initial liquid level exactly at the top of the electrodes. Hence there is translation invariance in the vertical direction and the contents are effectively a single 2D region, meaning that electrical conductivity can be modelled as a 2D field. The experimental set-up is depicted in Fig. 2.

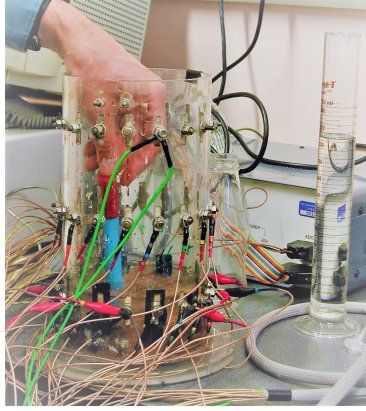


Figure 2: Experimental set-up: A cylindrical perspex tank containing tap water was stirred before an amount of potassium chloride was injected. Electrodes positioned around the tank measured voltages, which can be related through a partial differential equation to the internal conductivity field. The inverse problem consists of estimating the internal conductivity field from the voltages that were measured. (Only the bottom ring of electrodes were used for the data analysed in this paper.) Photo reproduced from West et al. (2005).

At the start of the experiment, a mixing impeller was used to create a rotational flow. This was then removed and, after a few seconds, concentrated potassium chloride solution was carefully injected into the tap water initially filling the tank. Data was then collected at regular time intervals until it was assumed that the liquid had fully mixed. Further details of the experiment can be found in West et al. (2005). These data were previously analysed (with non-probabilistic numerical methods) in Aykroyd & Cattle (2007).

This experiment mimics the situation when a hydrocyclone moves from an in-control regime to an out-of-control regime, in that initially there is a well defined core which gradually disappears as the liquids merge together. Performing the experiment in the laboratory allowed careful control of experimental conditions and, in particular, a lack of electrical interference from other equipment. A similar experimental set-up for data-generation was recently employed in Hyvonen & Leinonen (2015).

There are several widely accepted data collection ‘protocols’ for EIT (D 1986). A protocol specifies the sequence of electrodes that are used to create the electric field, as well as the sequence of electrodes used to measure the resulting electric potential. In this experiment the ‘reference protocol’ was used, where a drive current is passed between a reference electrode and each of the other electrodes in turn allowing a maximum of $m' = 7$ linearly independent current patterns. For each current pattern, the U_1, \dots, U_m were measured up to a common additive constant³, so that without loss of generality E_1 is the ‘reference’ electrode and $U_1 \equiv 0$. This permits a total of $7 \times 7 = 49$ measurements $y_{\cdot, k}$, obtained at each time point t_k in the experiment.

³This reflects the fact that it is voltage that is actually measured, which is the difference of two potentials.

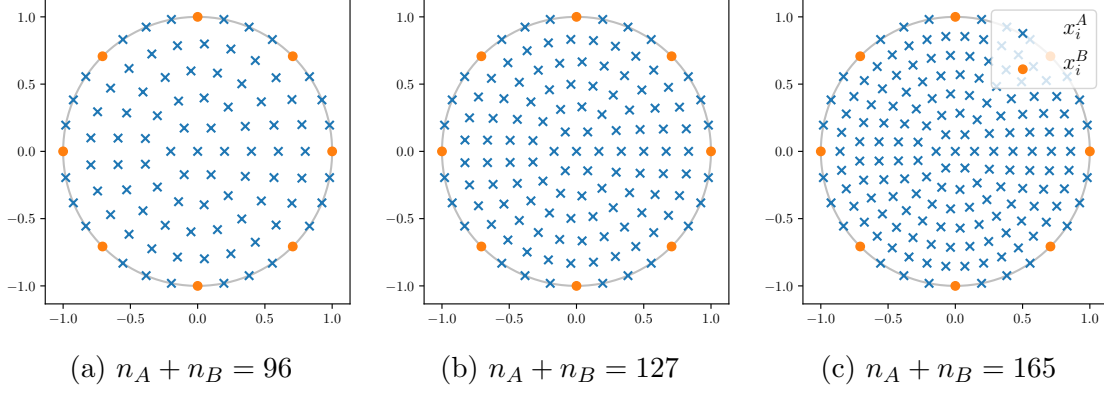


Figure 3: Typical sets of collocation points x_i^A and x_i^B that were used to discretise the PDE.

3.2 Experimental Results

The proposed statistical approach, based on probabilistic numerical methods, was used to make inferences on the unknown conductivity field a^\dagger based on this realistic experimental dataset. In this paper the contact impedances were considered to be negligible ($\zeta_i = 0$), but only to reduce the number of degrees of freedom in the assessment.

The assumption that k_u^0 has two continuous derivatives is sufficient for the prior to be well-defined (Prop. 3). However, the theoretical result in Prop. 4 requires that a more regular kernel with $\beta > 2 + d/2$ (weak) derivatives to ensure contraction of the (static) posterior. In reality, molecular diffusion implies that clear boundaries are not expected to be present in the true conductivity field. Thus it is reasonable to assume that both the conductivity field a and the electrical potential u will be fairly smooth in the interior D . For these reasons, the kernels employed for experiments below were of squared-exponential form, since this trivially meets all smoothness requirements, including smoothness of the solution u in D .

3.2.1 Static Recovery Problem

First, we calibrated our probabilistic numerical methods by analysing the static recovery problem. A prior model was placed on $\log a(\cdot, t)$ to ensure positivity. This prior was taken to be Gaussian, with a mean of zero and a squared-exponential covariance function

$$k_a(\mathbf{x}, \mathbf{x}') := \theta_a \exp\left(-\frac{\|\mathbf{x} - \mathbf{x}'\|_2^2}{2\ell_a^2}\right)$$

where θ_a controls the magnitude of fields drawn from the prior, while the length-scale ℓ_a controls how rapidly those functions vary. Since the main aim here is to assess the probabilistic meshless method, we simply fixed $\theta_a = 1$ and $\ell_a = 0.3$. Note that while it is common in EIT problems to use priors which promote hard edges in drawn samples, owing to applications in medicine, here a smooth prior is appropriate. For all experiments in this

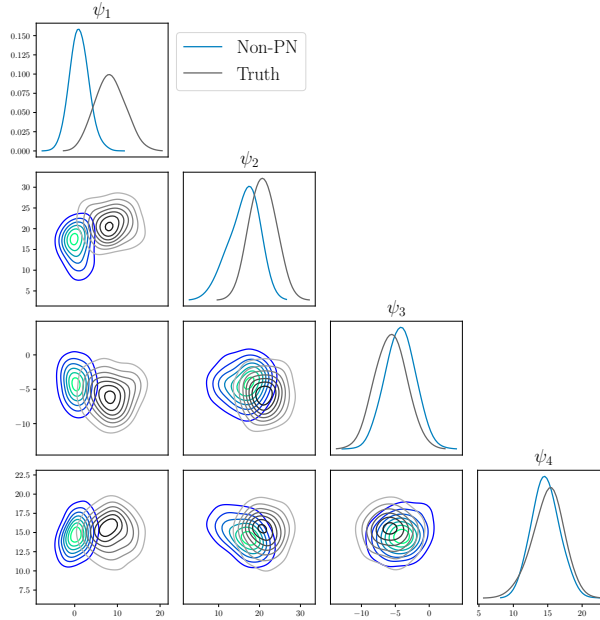


Figure 4: Failure case: Here a small number $n_A + n_B = 71$ of collocation points was used to discretise the PDE, but the uncertainty due to discretisation was not modelled. The reference posterior distribution over the coefficients ψ_i is plotted (grey) and compared to the approximation to the posterior obtained when the PDE is discretised (blue) and the discretisation error is not modelled (“Non-PN”). It is observed that the approximated posterior is highly biased.

paper the parameter σ , that describes technical measurement error, was set to $\sigma = 1.0$ based on analysis of a technical replicate dataset. For the Markov transition kernel we employed pre-conditioned the Crank Nicholson method that has been shown to be well-defined in the Hilbert space context Cotter et al. (2013).

For the probabilistic meshless method the prior model was centered and a squared-exponential covariance function was used, with $\theta_u = 100$ to match the scale of measurements in the dataset, and $\ell_u = 0.3007$, a value chosen by empirical Bayes based upon a high-quality reference sample. The collocation points were chosen on concentric circles, as shown in Fig. 3 for increasing values of n_A and n_B .

For illustration, we first considered simulated data and a coarse collocation method which did *not* model discretisation error. This was compared to a reference posterior, obtained using a brute-force symmetric collocation forward solver with a large number of collocation points. The result, shown in Fig. 4, was a posterior that did not contain the true data-generating field a^\dagger in its region of support. This result is typical (c.f. Sec. 2.2.3) and motivates the formal uncertainty quantification for discretisation error that is provided by probabilistic numerical methods in this paper.

The experimental data used for this assessment were obtained as a single frame (time point 14) from the larger temporal dataset. In Fig. 5(a) we show the posterior mean esti-

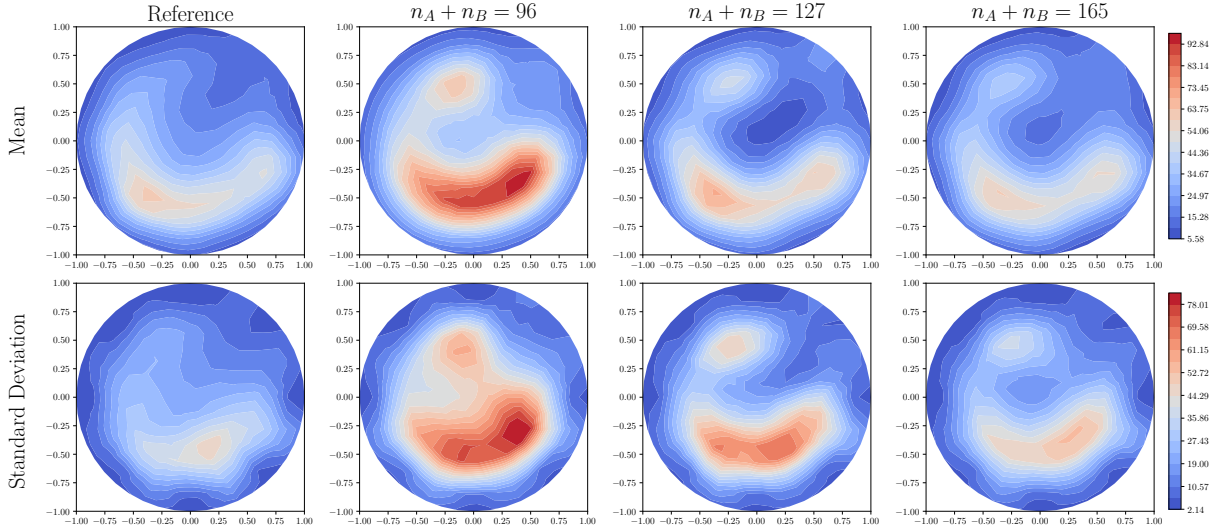


Figure 5: Posterior means and standard-deviations for the recovered conductivity field. The first column represents the reference solution, obtained using a symmetric collocation forward solver with a large number of collocation points. The remaining columns represent the recovered field when probabilistic numerical methods are used based on $n_A + n_B$ collocation points as shown in Fig. 3.

mate, together with its posterior variance, for a reference conductivity field generated using a high-quality symmetric collocation forward solver with $n_A + n_B = 207$ collocation points. Adjacent, in Fig. 5(b-d) we show the posterior mean and variance for the conductivity field obtained with probabilistic numerical methods for increasing values of n_A and n_B . It is seen that both the posterior mean and posterior standard deviation produced with the probabilistic numerical method converge to the reference posterior as the number of collocation points is increased. However, at coarse resolution, the posterior variance is inflated to reflect the contribution of a discretisation uncertainty to each numerical solution of the forward problem. This provides automatic protection against the erroneous results seen in Fig. 4.

In Fig. 6 we plot the number $n_A + n_B$ of collocation basis points versus the integrated posterior standard-deviation for the unknown conductivity field. These results demonstrate the computation-precision trade-off that is made possible with probabilistic numerical methods, and are consistent with the preliminary investigation in Cockayne et al. (2016a,b). Next, we turn to the temporal problem that motivates this research.

3.2.2 Temporal Recovery Problem

For this experiment, data were obtained at 49 regular time intervals. Times 1-10 were obtained before injection of the potassium chloride solution, while the injection occurred rapidly, between frames 10 and 11. The remaining time points 12-49 capture the diffusion and rotation of the liquids, which is the behaviour that we hope to recover.

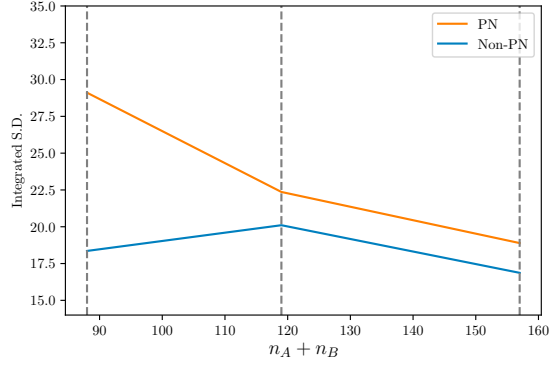


Figure 6: Posterior standard-deviation for the conductivity field, integrated over the domain D , as a function of the number $n_A + n_B$ of collocation points. The blue curve represents the standard case where error due to discretisation of the PDE is not quantified (“Non-PN”) whilst the red curve represents the case where a probabilistic numerical method is used to provide uncertainty quantification for the PDE solution itself (“PN”).

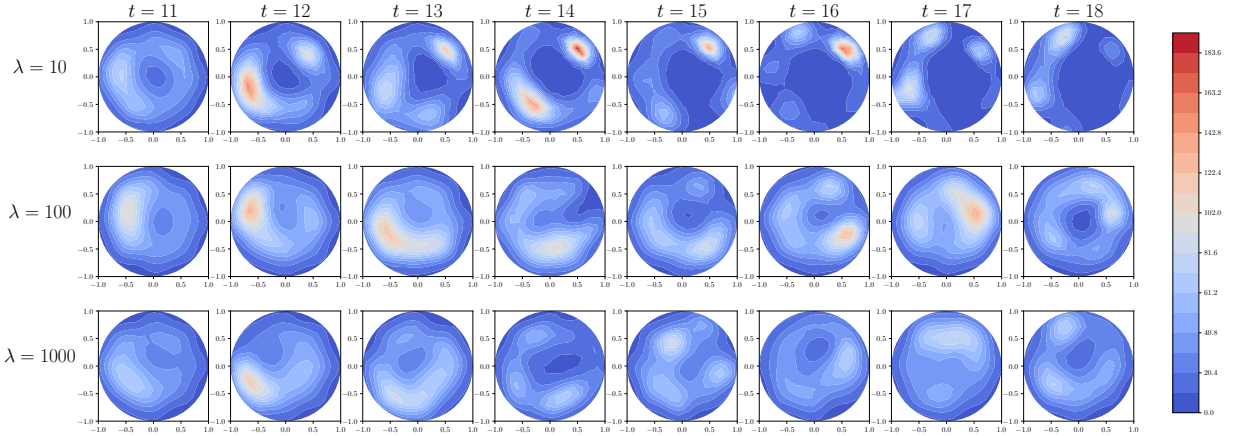


Figure 7: Posterior mean for the conductivity field $a(\cdot, t)$, shown as a function of the time index. Here we consider the dependence of the recovered field on the choice of the temporal covariance parameter λ .

The parameter λ controls the temporal smoothness of the conductivity field in the prior model. Three fixed values, $\lambda \in \{10, 100, 1000\}$ were considered in turn, representing increasing levels of smoothness. Our method was applied to estimate the time-evolution of the field. Results are shown in Fig. 7. The counter-clockwise rotation of the fluid was clearly seen for $\lambda = 100$, whilst the values $\lambda \in \{10, 1000\}$ represented too much and too little (respectively) temporal regularisation, which caused this information to be lost.

To assess whether the problems of bias and over-confidence due to discretisation can be mitigated in the temporal context, where discretisation errors are propagated and accumulate over time, we fixed $\lambda = 100$ and inspected the posterior over the coefficients ψ_i

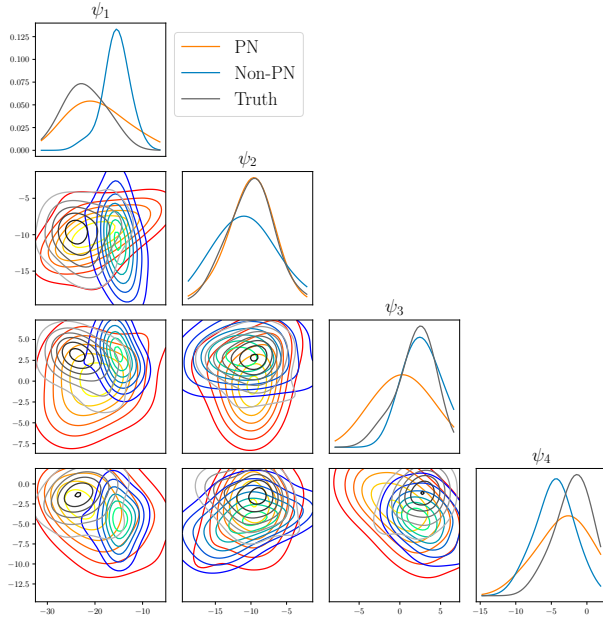


Figure 8: Posterior distribution over the coefficients ψ_i , at the final time point t_n . Here a small number $n_A + n_B = 71$ of collocation points was used to discretise the PDE. The reference posterior distribution over the coefficients ψ_i is plotted (grey) and compared to the approximation to the posterior obtained when discretisation of the PDE is not modelled (“Non-PN”) and modelled (“PN”).

at the final time point t_n . Results in Fig. 8 confirmed that the posterior Π_n^* (red) contains the true posterior Π_n (grey) in its effective support. On the other hand, the standard approximate posterior (blue), in which discretisation error is not modelled, was biased and over-confident. This provides empirical evidence to support the use of the proposed posterior Π_n^* .

In Fig. 9 we again plot the number $n_A + n_B$ of collocation basis points versus the integrated posterior standard-deviation for the unknown conductivity field, again at the final time point. These results demonstrate a computation-precision trade-off similar to that which was observed for the static recovery problem. Compared to the static recovery problem in Fig. 6, however, we observed greater inflation of the posterior standard-deviation when probabilistic numerical methods were used. This reflects the fact that we have constructed a full probability model for the effect of discretisation error, which is able to capture how these errors propagate and accumulate within the computational output.

4 Discussion

The motivation for this research was industrial process monitoring, but the associated methodological development was general. In particular, we addressed the important topic of how to perform uncertainty quantification for numerical error due to discretisation of

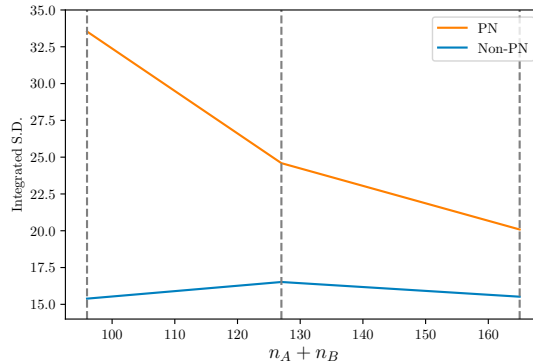


Figure 9: Posterior standard-deviation for the conductivity field $a(\cdot, t_n)$ at the final time point t_n , integrated over the domain D .

the physical governing equations specified through a PDE. Typically this source of error is ignored, or its contribution bounded through detailed numerical analysis, such as Schwab & Stuart (2012). However, in the temporal setting, theoretical bounds are difficult to obtain due to propagation and accumulation of errors, so that it is unclear how to proceed.

In this work we proposed a statistical solution, wherein a probabilistic numerical method was used to provide uncertainty quantification for the discretisation error associated with a collocation-type numerical method. Aided by sequential Monte Carlo sampling methods, it was shown how this model for *discretisation uncertainty* can be employed in the temporal context. The result was a full quantification of uncertainty, that accounts for both statistical uncertainty and for propagation and accumulation of discretisation uncertainty in the final output. For our motivating industrial application, this work is expected to facilitate more reliable anticipation and pro-active control of the hydrocyclone, to ensure safety in operation (Bradley 2013).

The methods that we pursued differ in a fundamental sense to techniques that seek to *emulate* the forward model. Emulation, as well as dimension reduction methods, have been widely used in static recovery problems to reduce the computational cost of repeatedly solving the governing PDE (Marzouk et al. 2007, Marzouk & Najm 2009, Cotter et al. 2010, Schwab & Stuart 2012, Cui et al. 2016, Chen & Schwab 2016*c,b*). Notably Stuart & Teckentrup (2016), Calvetti et al. (2017) considered integrating the emulator uncertainty into inference for model parameters. However, to train an emulator it is usually required to have access to a training set of parameters a for which the exact solution u of the PDE is provided. Thus the focus of emulation is related to generalisation in the a domain, as opposed to quantification of discretisation uncertainty in the u domain. An interesting extension of this work would be to combine these two complementary techniques; this would be expected to reduced the computational cost of the proposed method.

The principal limitation of our approach was that a Markov temporal evolution of the conductivity field $a(\cdot, t)$ was assumed. Physical consideration suggest that the Markov assumption is incorrect, since time-derivatives of all orders of this field will vary continuously

and thus encode information that is useful. However, it is not clear how this information can be encoded into a prior for the temporal evolution of the conductivity field whilst preserving the computationally convenient filtering framework. On the other hand, the Markov prior can be statistically justified in that it represents an encoding of partial prior information Potter & Anderson (1983). It remains a problem for future work to investigate the potential loss of estimator efficiency as a result of encoding only partial information into the prior model.

The second limitation we highlight is that the prior model for the potential field $u(\cdot, t)$ did not include a temporal component. This choice was algorithmically convenient, as it de-coupled each of the forward problems of solving the PDE, such that each time a probabilistic numerical method was called, it could be implemented “out of the box”. Nevertheless, a temporal covariance structure in the parameter a implies that there also exists such structure in u and the effect of not encoding this aspect of prior information should be further investigated.

Overall, we are excited by the prospect of new and more powerful methods for uncertainty quantification that can deal with both statistical and discretisation error in a unified analytical framework.

References

- Aykroyd, R. G. (2015), *Industrial Tomography: Systems and Applications*, Woodhead Publishing, chapter Statistical Image Reconstruction, pp. 401–428.
- Aykroyd, R. G. & Cattle, B. A. (2007), ‘A boundary-element approach for the complete-electrode model of EIT illustrated using simulated and real data’, *Inverse Problems in Science and Engineering* **15**(5), 441–461.
- Beskos, A., Jasra, A., Muzaffer, E. A. & Stuart, A. M. (2015), ‘Sequential Monte Carlo methods for Bayesian elliptic inverse problems’, *Statistics and Computing* **25**(4), 727–737.
- Bradley, D. (2013), *The Hydrocyclone: International Series of Monographs in Chemical Engineering*, Vol. 4, Elsevier.
- Briol, F.-X., Oates, C. J., Girolami, M., Osborne, M. A. & Sejdinovic, D. (2016), ‘Probabilistic integration: A role for statisticians in numerical analysis?’, *arXiv:1512.00933*.
- Bui-Thanh, T. & Ghattas, O. (2014), ‘An analysis of infinite dimensional Bayesian inverse shape acoustic scattering and its numerical approximation’, *SIAM/ASA Journal on Uncertainty Quantification* **2**(1), 203–222.
- Calvetti, D., Dunlop, M. M., Somersalo, E. & Stuart, A. M. (2017), ‘Iterative updating of model error for bayesian inversion’, *arXiv:1707.04246*.

- Chen, P. & Schwab, C. (2015), ‘Sparse-grid, reduced-basis Bayesian inversion’, *Computer Methods in Applied Mechanics and Engineering* **297**, 84–115.
- Chen, P. & Schwab, C. (2016a), Adaptive sparse grid model order reduction for fast Bayesian estimation and inversion, in ‘Sparse Grids and Applications (Stuttgart 2014)’, Springer, pp. 1–27.
- Chen, P. & Schwab, C. (2016b), ‘Model order reduction methods in computational uncertainty quantification’, *Handbook of Uncertainty Quantification*, Springer .
- Chen, P. & Schwab, C. (2016c), ‘Sparse-grid, reduced-basis Bayesian inversion: Nonaffine-parametric nonlinear equations’, *Journal of Computational Physics* **316**, 470–503.
- Cheng, K.-S., Isaacson, D., Newell, J. C. & Gisser, D. G. (1989), ‘Electrode models for electric current computed tomography’, *IEEE Transactions on Biomedical Engineering* **36**(9), 918–924.
- Chkrebtii, O. A., Campbell, D. A., Calderhead, B. & Girolami, M. A. (2016), ‘Bayesian solution uncertainty quantification for differential equations’, *Bayesian Analysis* **11**(4), 1239–1267.
- Chopin, N. (2002), ‘A sequential particle filter method for static models’, *Biometrika* **89**(3), 539–552.
- Cialenco, I., Fasshauer, G. E. & Ye, Q. (2012), ‘Approximation of stochastic partial differential equations by a kernel-based collocation method’, *International Journal of Computer Mathematics* **89**(18), 2543–2561.
- Cockayne, J., Oates, C., Sullivan, T. & Girolami, M. (2016a), ‘Probabilistic meshless methods for Bayesian inverse problems’, *arXiv:1605.07811* .
- Cockayne, J., Oates, C., Sullivan, T. & Girolami, M. (2016b), Probabilistic numerical methods for PDE-constrained Bayesian inverse problems, in G. Verdoolaege, ed., ‘Proceedings of the 36th International Workshop on Bayesian Inference and Maximum Entropy Methods in Science and Engineering’, Vol. 1853 of *AIP Conference Proceedings*.
- Conrad, P. R., Girolami, M., Särkkä, S., Stuart, A. & Zygalakis, K. (2017), ‘Statistical analysis of differential equations: Introducing probability measures on numerical solutions’, *Statistics and Computing* **27**(4), 1065–1082.
- Cotter, S. L., Dashti, M. & Stuart, A. M. (2010), ‘Approximation of Bayesian inverse problems for PDEs’, *SIAM Journal on Numerical Analysis* **48**(1), 322–345.
- Cotter, S. L., Roberts, G. O., Stuart, A. M., White, D. et al. (2013), ‘MCMC methods for functions: Modifying old algorithms to make them faster’, *Statistical Science* **28**(3), 424–446.

- Cui, T., Marzouk, Y. & Willcox, K. (2016), ‘Scalable posterior approximations for large-scale Bayesian inverse problems via likelihood-informed parameter and state reduction’, *Journal of Computational Physics* **315**, 363–387.
- D, I. (1986), ‘Distinguishability of conductivity by electric current computed tomography’, *IEEE Trans. Med. Imaging* **MI-5**, No. 2, 91–95.
- Dashti, M. & Stuart, A. M. (2016), *Handbook of Uncertainty Quantification*, Springer, chapter The Bayesian approach to inverse problems, pp. 311–428.
- Del Moral, P. (2004), *Feynman-Kac Formulae*, Springer.
- Dunlop, M. M. & Stuart, A. M. (2016), ‘The Bayesian formulation of EIT: Analysis and algorithms’, *Inverse Problems and Imaging* **10**(4), 1007–1036.
- Fasshauer, G. E. (1996), Solving partial differential equations by collocation with radial basis functions, in A. L. Méhauté, C. Rabut & L. L. Schumaker, eds, ‘Surface Fitting and Multiresolution Methods. Vol. 2 of the Proceedings of the 3rd International Conference on Curves and Surfaces held in Chamonix-Mont-Blanc, June 27-July 3’, Vanderbilt University Press, Nashville, TN, pp. 131–178.
- Gerber, M. & Chopin, N. (2015), ‘Sequential quasi Monte Carlo’, *Journal of the Royal Statistical Society: Series B* **77**(3), 509–579.
- Gross, L. (1967), Abstract Wiener spaces, in ‘Proceedings of the Fifth Berkeley Symposium on Mathematical Statistics and Probability, Volume 2: Contributions to Probability Theory, Part 1’, The Regents of the University of California.
- Gutierrez, J., Dyakowski, T., Beck, M. & Williams, R. (2000), ‘Using electrical impedance tomography for controlling hydrocyclone underflow discharge’, *Powder Technology* **108**(2), 180–184.
- Hennig, P., Osborne, M. A. & Girolami, M. (2015), Probabilistic numerics and uncertainty in computations, in ‘Proceedings of the Royal Society A’, Vol. 471, The Royal Society.
- Hyvonen, N. & Leinonen, M. (2015), ‘Stochastic Galerkin finite element method with local conductivity basis for electrical impedance tomography’, *SIAM/ASA Journal on Uncertainty Quantification* **3**(1), 998–1019.
- Kaipio, J. P., Kolehmainen, V., Somersalo, E. & Vauhkonen, M. (2000), ‘Statistical inversion and Monte Carlo sampling methods in electrical impedance tomography’, *Inverse Problems* **16**(5), 1487.
- Kaipio, J. P., Kolehmainen, V., Vauhkonen, M. & Somersalo, E. (1999), ‘Inverse problems with structural prior information’, *Inverse Problems* **15**(3), 713.

- Kantas, N., Beskos, A. & Jasra, A. (2014), ‘Sequential Monte Carlo methods for high-dimensional inverse problems: A case study for the Navier–Stokes equations’, *SIAM/ASA Journal on Uncertainty Quantification* **2**(1), 464–489.
- Kennedy, M. C. & O’Hagan, A. (2001), ‘Bayesian calibration of computer models’, *Journal of the Royal Statistical Society: Series B (Statistical Methodology)* **63**(3), 425–464.
- Law, K., Stuart, A. & Zygalakis, K. (2015), *Data Assimilation: A Mathematical Introduction*, Vol. 62, Springer.
- Loève, M. (1977), ‘Probability theory’.
- Lord, G., Powell, C. & Shardlow, T. (2014), *An introduction to computational stochastic PDEs*, number 50, Cambridge University Press.
- Marzouk, Y. M. & Najm, H. N. (2009), ‘Dimensionality reduction and polynomial chaos acceleration of Bayesian inference in inverse problems’, *Journal of Computational Physics* **228**(6), 1862–1902.
- Marzouk, Y. M., Najm, H. N. & Rahn, L. A. (2007), ‘Stochastic spectral methods for efficient Bayesian solution of inverse problems’, *Journal of Computational Physics* **224**(2), 560–586.
- Marzouk, Y. & Xiu, D. (2009), ‘A stochastic collocation approach to Bayesian inference in inverse problems’, *Communications in Computational Physics* **6**(4), 826–847.
- Nagel, J. B. & Sudret, B. (2016), ‘Spectral likelihood expansions for Bayesian inference’, *Journal of Computational Physics* **309**, 267–294.
- Nouy, A. & Soize, C. (2014), ‘Random field representations for stochastic elliptic boundary value problems and statistical inverse problems’, *European Journal of Applied Mathematics* **25**(03), 339–373.
- Novak, E. & Wozniakowski, H. (2008), *Tractability of Multivariate Problems. Vol. I: Linear Information*, Vol. 6 of *EMS Tracts in Mathematics*, European Mathematical Society (EMS), Zürich.
- Novak, E. & Wozniakowski, H. (2010), *Tractability of Multivariate Problems. Vol II: Standard Information for Functionals*, Vol. 12 of *EMS Tracts in Mathematics*, European Mathematical Society (EMS), Zürich.
- Owhadi, H. (2015), ‘Bayesian numerical homogenization’, *Multiscale Modeling & Simulation* **13**(3), 812–828.
- Owhadi, H. (2017), ‘Multi-grid with rough coefficients and multiresolution operator decomposition from hierarchical information games’, *SIAM Review* **59**(1), 99–149. To appear.

- Owhadi, H. & Zhang, L. (2017), ‘Gambllets for opening the complexity-bottleneck of implicit schemes for hyperbolic and parabolic ODEs/PDEs with rough coefficients’, *Journal of Computational Physics* **347**, 99–128.
- Polydorides, N. & Lionheart, W. R. (2002), ‘A MATLAB toolkit for three-dimensional electrical impedance tomography: A contribution to the Electrical Impedance and Diffuse Optical Reconstruction Software project’, *Measurement Science and Technology* **13**(12), 1871.
- Potter, J. & Anderson, B. (1983), ‘Statistical inference with partial prior information’, *IEEE Transactions on Information Theory* **29**(5), 688–695.
- Quarteroni, A. & Valli, A. (2008), *Numerical Approximation of Partial Differential Equations*, Springer Science & Business Media.
- Raissi, M., Perdikaris, P. & Karniadakis, G. (2017), ‘Inferring solutions of differential equations using noisy multi-fidelity data’, *Journal of Computational Physics* **335**, 736–746.
- Särkkä, S. (2013), *Bayesian Filtering and Smoothing*, Vol. 3, Cambridge University Press.
- Schillings, C. & Schwab, C. (2013), ‘Sparse, adaptive Smolyak quadratures for Bayesian inverse problems’, *Inverse Problems* **29**(6), 065011.
- Schillings, C. & Schwab, C. (2014), ‘Sparsity in Bayesian inversion of parametric operator equations’, *Inverse Problems* **30**(6), 065007.
- Schwab, C. & Stuart, A. M. (2012), ‘Sparse deterministic approximation of Bayesian inverse problems’, *Inverse Problems* **28**(4), 045003.
- Somersalo, E., Cheney, M. & Isaacson, D. (1992), ‘Existence and uniqueness for electrode models for electric current computed tomography’, *SIAM Journal on Applied Mathematics* **52**(4), 1023–1040.
- Sripriya, R., Kaulaskar, M., Chakraborty, S. & Meikap, B. (2007), ‘Studies on the performance of a hydrocyclone and modeling for flow characterization in presence and absence of air core’, *Chemical Engineering Science* **62**(22), 6391–6402.
- Steinwart, I. & Christmann, A. (2008), *Support Vector Machines*, Springer Science & Business Media.
- Stuart, A. M. (2010), ‘Inverse problems: A Bayesian perspective’, *Acta Numerica* **19**, 451–559.
- Stuart, A. M. & Teckentrup, A. L. (2016), ‘Posterior consistency for Gaussian process approximations of Bayesian posterior distributions’, *arXiv:1603.02004* .

- Sullivan, T. J. (2015), *Introduction to Uncertainty Quantification*, Vol. 63 of *Texts in Applied Mathematics*, Springer.
- Todescato, M., Carron, A., Carli, R., Pillonetto, G. & Schenato, L. (2017), ‘Efficient spatio-temporal Gaussian regression via Kalman filtering’, *arXiv:1705.01485*.
- Vauhkonen, M., Lionheart, W. R., Heikkinen, L. M., Vauhkonen, P. J. & Kaipio, J. P. (2001), ‘A MATLAB package for the EIDORS project to reconstruct two-dimensional EIT images’, *Physiological Measurement* **22**(107).
- Watzenig, D. & Fox, C. (2009), ‘A review of statistical modelling and inference for electrical capacitance tomography’, *Measurement Science and Technology* **20**(5), 052002.
- Wendland, H. (2005), *Scattered Data Approximation*, Vol. 17 of *Cambridge Monographs on Applied and Computational Mathematics*, Cambridge University Press.
- Werschulz, A. G. (1996), ‘The complexity of definite elliptic problems with noisy data’, *Journal of Complexity* **12**(4), 440–473.
- West, R. M., Meng, S., Aykroyd, R. G. & Williams, R. A. (2005), ‘Spatial-temporal modeling for electrical impedance imaging of a mixing process’, *Review of Scientific Instruments* **76**(7), 073703.
- Wiener, N. (1949), *Extrapolation, Interpolation, and Smoothing of Stationary Time Series*, MIT Press Cambridge.
- Yan, L. & Guo, L. (2015), ‘Stochastic collocation algorithms using ℓ_1 -minimization for Bayesian solution of inverse problems’, *SIAM Journal on Scientific Computing* **37**(3), A1410–A1435.